Experimental search for nonfusion yield in the heavy residues emitted in the $^{11}B + {}^{12}C$ reaction

J. F. Mateja
Physics Department, Tennessee Technological University, Cookeville, Tennessee 38505

A. D. Frawley, R. A. Parker, and K. Sartor
Physics Department, Florida State University, Tallahassee, Florida 32306
(Received 3 June 1985; revised manuscript received 17 January 1986)

The mechanism responsible for fusion cross section limitations in light heavy-ion systems has been the focus of numerous experimental and theoretical studies. Many of the experimental investigations have involved a study of the heavy residues emitted following the interaction of light heavy ions. One difficulty encountered in such studies is separating events from competing reaction mechanisms, such as direct transfer and incomplete fusion, from fusion-evaporation events. In the present work, direct and reverse reaction kinematics are exploited in an effort to determine the magnitude of the nonfusion strength in the heavy residue spectra for the interaction of ^{11}B and ^{12}C. It is particularly important that the $^{11}B+{}^{12}C$ fusion strength be properly identified, as it is the measured fusion strength in this entrance channel which in earlier studies clearly ruled out a fusion cross section limitation based upon having reached a critical density of compound nuclear states. In agreement with the earlier investigations, the present study reveals no significant nonfusion component in the heavy residue spectra for the $^{11}B+{}^{12}C$ reaction.

I. INTRODUCTION

Over the past ten years considerable experimental and theoretical work has been directed toward understanding the cause of fusion cross section limitations for reactions which involve nuclei in the $2s$-$1p$ shell.[1-11] Early investigations suggested that at some energy above the Coulomb barrier a limitation was brought about because a critical density of compound nucleus states, the compound nucleus yrast or "statistical" yrast line, had been reached.[5-7] Recent studies of the ^{23}Na compound nucleus, however, suggest that long before a compound nucleus related limitation occurs, a limitation arises which results from the competition between fusion and other entrance channel dependent reaction processes.[9-11] This conclusion was based on a study of the fusion cross sections for four entrance channels which form the ^{23}Na compound nucleus, $^{11}B+{}^{12}C$, $^{10}B+{}^{13}C$, $^{7}Li+{}^{16}O$, and $^{9}Be+{}^{14}N$.[11] After extracting the critical angular momenta from the experimentally measured fusion cross sections in the above systems, a comparison of the critical angular momenta as a function of ^{23}Na excitation energy reveals that three of the entrance channels ($^{10}B+{}^{13}C$, $^{7}Li+{}^{16}O$, and $^{9}Be+{}^{14}N$) appear to approach a common limitation as shown in Fig. 1. Such a result has been interpreted in studies like those in Refs. 5–7 as a signature that a critical density of states has been reached in the compound nucleus. However, the critical angular momentum line for the fourth entrance channel, the $^{11}B+{}^{12}C$, does not approach the same line as the others. It is implied that $^{11}B+{}^{12}C$ fusion cross sections are not as severely limited as are the fusion cross sections for the other three entrance channels. It is the $^{11}B+{}^{12}C$ entrance channel which brings in the highest angular momentum at the lowest compound nucleus energy and which should, therefore, be the entrance channel which is most severely limited by a mechanism involving a critical density of compound nuclear states. There are two possible explanations: (1) yield in the heavy residue exit channels of $^{11}B+{}^{12}C$ which was attributed to fusion actually arises from some other reaction mechanism, producing erroneously large $^{11}B+{}^{12}C$ fusion cross sections, or (2) the limitation in this energy region is not brought about because a critical density of states has been reached in the compound nucleus.

The purpose of the present work was to subject the heavy residues which result from the $^{11}B+{}^{12}C$ interaction to a specific experimental test to determine whether or not the residues do indeed result from fusion evaporation through the ^{23}Na compound nucleus, as assumed in the earlier investigations.[9-11] Of particular concern is the possible presence of direct transfer and incomplete fusion

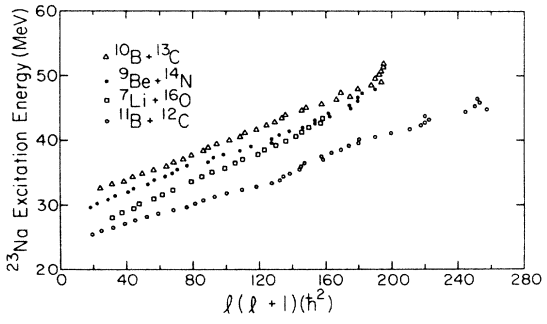

FIG. 1. A comparison of the critical angular momenta for the $^{11}B+{}^{12}C$, $^{10}B+{}^{13}C$, $^{9}Be+{}^{14}N$, and $^{7}Li+{}^{16}O$ entrance channels as a function of compound nucleus excitation energy. These results were taken from Ref. 11.

strength. The test which is employed in the present work exploits the fact that in a nearly symmetric system such as $^{11}B+^{12}C$, the laboratory energy of the fusion products is essentially independent of which entrance channel nucleus is used as the target and which is used as the projectile, while the energy of direct transfer and incomplete fusion products depends strongly on which nucleus is the target or projectile. A careful, mass-by-mass comparison of the heavy residue energy spectra has been made for the two reactions $^{12}C(^{11}B,X)$ and $^{11}B(^{12}C,X)$. If there is any significant direct transfer or incomplete fusion strength, it will appear at substantially different energies in the energy spectra of the above two reactions.

The discussion of the experimental details is presented in Sec. II of this paper. A comparison of the residues which result from the $^{12}C(^{11}B,X)$ and $^{11}B(^{12}C,X)$ reactions is made in Sec. III. Our conclusions are presented in Sec. IV.

II. EXPERIMENTAL PROCEDURE

The ^{12}C and ^{11}B beams for the experiment were provided by the Florida State University super-FN tandem Van de Graaff accelerator. So that the same compound nucleus excitation energy would be reached, the $^{12}C(^{11}B,X)$ and $^{11}B(^{12}C,X)$ reactions were studied at the same center-of-mass energy, $E_{c.m.}=25$ MeV. Laboratory bombarding energies of 48 and 52.36 MeV were required for the ^{11}B and ^{12}C projectiles, respectively.

For the two reactions, self-supporting ^{12}C and ^{11}B targets were used. While no significant contamination of the ^{12}C target was observed, ^{16}O was present on the ^{11}B target. To allow a proper contaminant subtraction, the residues from the $^{16}O(^{12}C,X)$ reaction were measured at 52.36 MeV for all of the angles studied in the $^{11}B(^{12}C,X)$ experiment. A contaminant subtraction was then made on a mass-by-mass basis.

The heavy reaction products, studied over an angular range from 5° to 25°, were mass identified by measuring flight times along a 2.7 m flight path. The system is comprised of a microchannel plate start detector and a silicon stop detector. Additional details related to this experimental setup can be found in Ref. 10. A typical two-dimensional mass versus energy spectrum is shown in Fig. 2.

The absolute cross sections for the present studies were determined by comparing the elastic scattering cross sections for $^{11}B+^{12}C$ scattering with the predictions of optical model calculations. The optical model parameters used in the present analysis were taken from our earlier investigations of $^{11}B+^{12}C$ elastic scattering in this energy region.[10] The calculated angular distributions and those measured in the present experiment are displayed in Fig. 3 (forward angles). The agreement is quite good. The uncertainty in the absolute cross section is estimated to be approximately 10%. This uncertainty takes into account counting statistics, angle setting uncertainties, extrapolation of the data to zero degrees and beyond 25°, and errors in measuring the absolute target thickness.

The relative cross section normalization of the two reactions could be checked because of a peculiar feature of

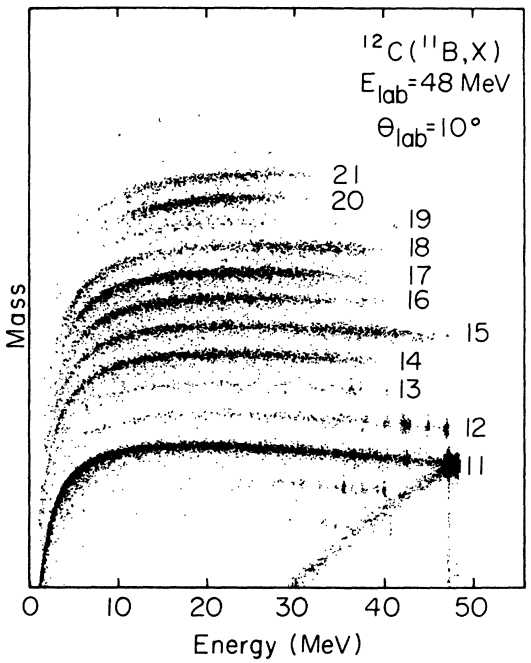

FIG. 2. A representative mass versus energy contour map for the $^{11}B+^{12}C$ system.

the $^{11}B+^{12}C$ reaction. A proton exchange between the target and projectile occurs which gives rise to a large, back-angle, transfer cross section in the elastic scattering channel.[12] The relative normalization between the two reactions could, therefore, be checked by comparing the proton pickup cross section in the $^{12}C(^{11}B,^{12}C)$ reaction with the proton stripping cross section in the $^{11}B(^{12}C,^{11}B)$ reaction. This comparison, made at the back angles, is shown in Fig. 3. As can be seen in Fig. 3, there is excellent agreement between the two sets of data.

III. EXPERIMENTAL RESULTS AND DISCUSSION

Of primary interest in attempting to identify nonfusion yield in this study are the shapes of the residue energy spectra for the two $^{11}B+^{12}C$ entrance channel configura-

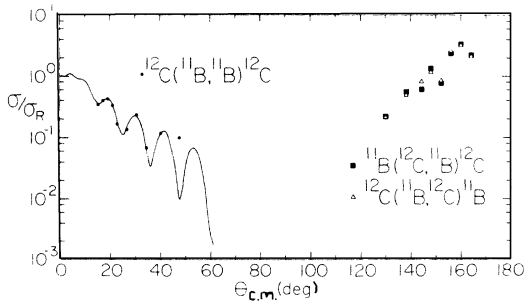

FIG. 3. Elastic scattering angular distributions for the $^{11}B+^{12}C$ entrance channel. The solid curve results from an optical model calculation using $^{11}B+^{12}C$ optical model parameters taken from Ref. 10. The increase in the back-angle elastic scattering yield results from a proton exchange between the target and the projectile.

tions. The observed energy of direct transfer and incomplete fusion products depends strongly on the entrance channel configuration, while the energy of the fusion-evaporation events does not. From simple classical considerations, it can be shown that the centroid energy for fusion-evaporation products is given by:

$$E_{\text{cent}} = \frac{M_r M_p E_p}{M_{\text{cn}}^2} \cos^2\theta_{\text{lab}} , \quad (1)$$

where M_r, M_p, and M_{cn} are the residue, projectile, and compound nucleus masses, respectively; E_p is the laboratory energy of the projectile; and θ_{lab} is the laboratory angle of the detected residue. As there is only a slight difference in projectile mass and bombarding energy between the two $^{11}B+^{12}C$ entrance channel configurations, only a small shift in the energy distribution ($\approx 20\%$) and little, if any, change in the shape of the fusion-evaporation energy spectrum would be expected. The energy of direct transfer or incomplete fusion products, on the other hand, will differ significantly depending on whether the major portion of the residue mass comes from the target or from the projectile.

Consider, for example, a process which leads to a mass 15 residue. From Eq. (1) the energy centroid of the mass 15 residue created through the fusion evaporation of a 48 MeV ^{11}B projectile with a ^{12}C target at 10° is 14.5 MeV. When the entrance channel configuration is inverted and a 52.36 MeV ^{12}C nucleus impinges on a ^{11}B target nucleus, the energy centroid at 10° shifts by 2.8 MeV to 17.3 MeV. For a process like triton transfer to ^{15}N, however, very different ^{15}N energies will be observed in the reaction depending upon whether the mechanism is triton stripping, $^{12}C(^{11}B,^{8}Be)^{15}N$, or triton pickup, $^{11}B(^{12}C,^{15}N)^{8}Be$. In the stripping case, the ^{15}N will have a recoil energy of approximately 2 MeV at 10° for a residual excitation energy of 5 to 10 MeV. In the pickup case, the ^{15}N energy at 10° will be around 46 MeV for a residual excitation energy of 5 to 10 MeV. Because of this drastic change in residue energy, the shape of the mass 15 energy spectra would change significantly, depending upon which particle was the projectile. It should also be kept in mind that a fairly substantial cross section reduction (approximately 26% or 270 mb of the previously measured $^{11}B+^{12}C$ fusion cross section) is required to bring the $^{11}B+^{12}C$ critical angular momentum line into agreement with those from the other three entrance channels at the energy being considered.[9–11] One is looking, therefore, for substantial shape differences in at least some of the energy spectra.

There is a complication which must be considered when evaluating the individual energy spectra. Consider again the triton transfer reaction discussed above. In actuality the $^{12}C(^{11}B,^{8}Be)^{15}N$ reaction can produce both high and low energy ^{15}N particles. A low energy ^{15}N particle results from the triton stripping reaction discussed above; the high energy ^{15}N residues are produced in the alpha pickup reaction $^{12}C(^{11}B,^{15}N)^{8}Be$. These high energy ^{15}N particles which arise by alpha pickup would then fall in the same region of the energy spectrum as the high energy ^{15}N residues which are produced in the triton pickup reaction, $^{11}B(^{12}C,^{15}N)^{8}Be$. Therefore, if the alpha pickup and

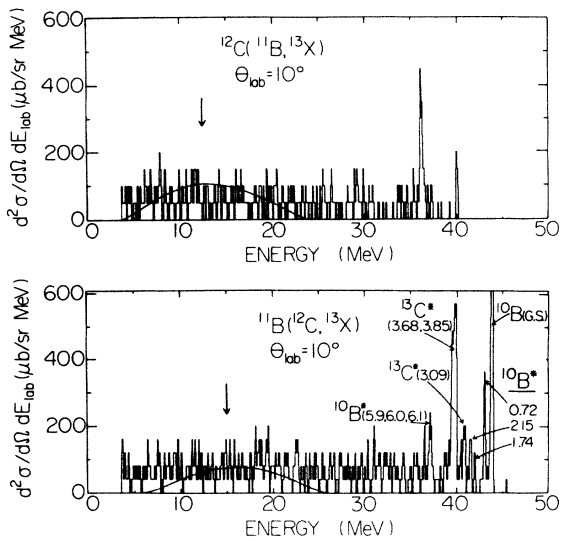

FIG. 4. A comparison of the mass 13 energy spectra for 48 MeV ^{11}B on ^{12}C (top) and 52.36 MeV ^{12}C on ^{11}B (bottom). The solid curves are the results of Hauser-Feshbach evaporation calculations. The arrows depict the centroid energies calculated using Eq. (1).

triton transfer cross sections were similar enough in magnitude, the ^{15}N energy spectra from the $^{12}C(^{11}B,^{15}N)$ and $^{11}B(^{12}C,^{15}N)$ reactions could look very similar, despite large direct transfer cross sections. However, to produce cross sections of the same magnitude and thereby produce similarly shaped energy spectra, the ^{12}C alpha particle spectroscopic factor would have to be similar to that of the triton spectroscopic factor in ^{11}B. We will return to this point later.

The residue energy spectra for the two entrance channel configurations are compared for masses 13–22 in Figs. 4–13, respectively. No comparison of the mass 11 and 12 energy spectra has been made because a strong inelastic

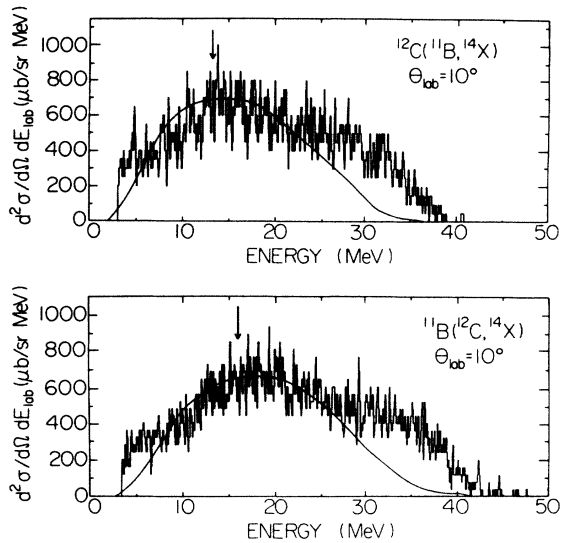

FIG. 5. A comparison of the mass 14 energy spectra for 48 MeV ^{11}B on ^{12}C (top) and 52.36 MeV ^{12}C on ^{11}B (bottom). See Fig. 4 for additional figure descriptions.

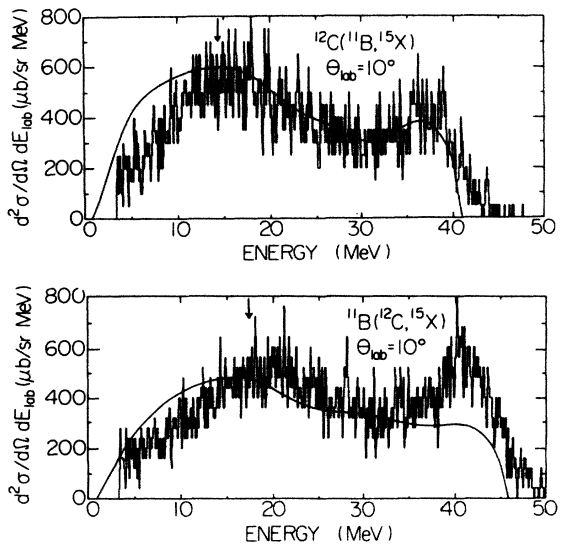

FIG. 6. A comparison of the mass 15 energy spectra for 48 MeV ^{11}B on ^{12}C (top) and 52.36 MeV ^{12}C on ^{11}B (bottom). See Fig. 4 for additional figure descriptions.

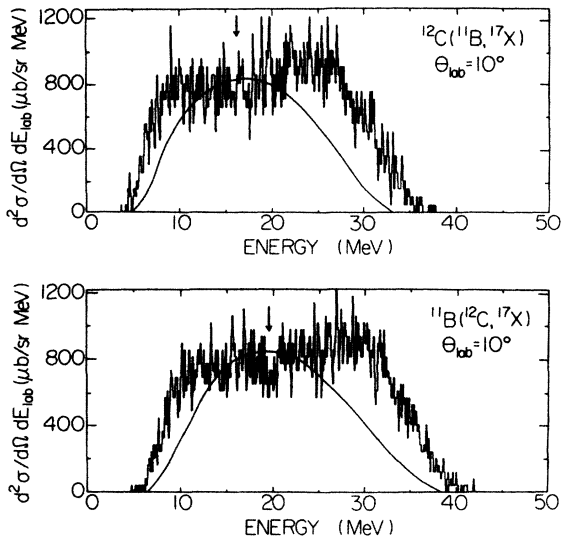

FIG. 8. A comparison of the mass 17 energy spectra for 48 MeV ^{11}B on ^{12}C (top) and 52.36 MeV ^{12}C on ^{11}B (bottom). See Fig. 4 for additional figure descriptions.

component completely masks the areas of interest in these mass groups (the mass 11 group was obscured in the ^{11}B induced reaction while the mass 12 group was obscured in the ^{12}C induced reaction). Also included in Figs. 4—13 are the locations of the fusion-evaporation energy centroids calculated using Eq. (1) (arrows) and the results of a Hauser-Feshbach calculation of the fusion-evaporation energy spectra (solid curves). For the Hauser-Feshbach calculation, the computer code LILITA has been used.[13]

The most striking feature of the experimental energy spectra shown in Figs. 4—13 is the strong similarity in the shapes of the energy spectra for a particular residue mass for the two entrance channel configurations. The fact that there are no large differences in the shapes of the experimental energy spectra suggests that no large direct transfer or incomplete fusion strength exists in these residue yields. As mass groups 13—22 contain essentially all of the previously reported fusion-evaporation yield, no change in the earlier total fusion cross section and, therefore, no change in the extracted critical angular momenta is required. This, of course, supports the contention that a critical density of compound nuclear states is not responsible for the fusion cross section limitations observed in the entrance channels which form the ^{23}Na compound nucleus.

While no large differences in the above energy spectra are apparent, there are slight differences in the residue energy spectra between the two entrance channel configura-

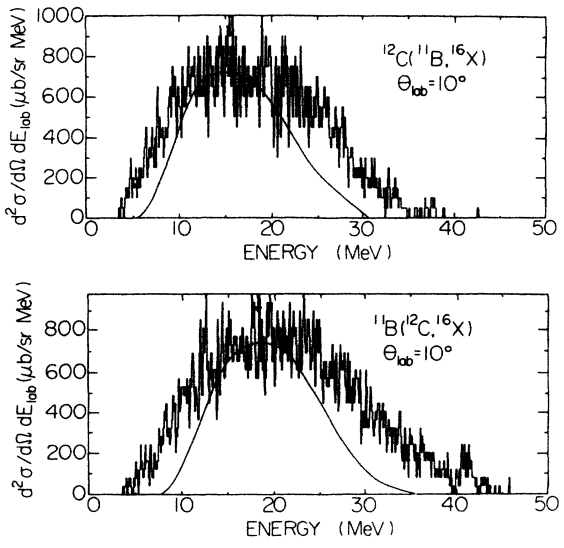

FIG. 7. A comparison of the mass 16 energy spectra for 48 MeV ^{11}B on ^{12}C (top) and 52.36 MeV ^{12}C on ^{11}B (bottom). See Fig. 4 for additional figure descriptions.

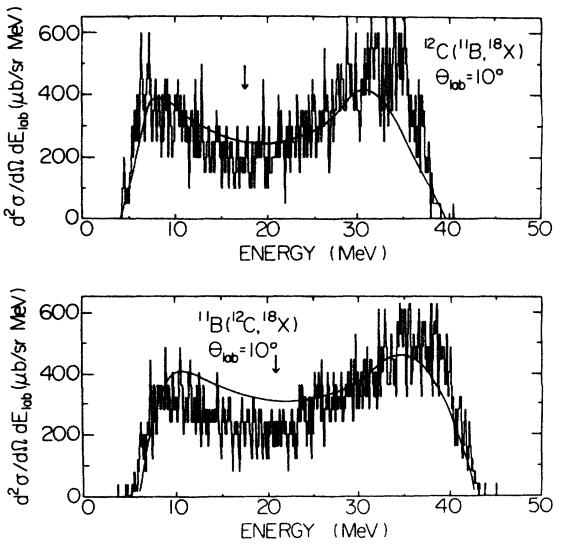

FIG. 9. A comparison of the mass 18 energy spectra for 48 MeV ^{11}B on ^{12}C (top) and 52.36 MeV ^{12}C on ^{11}B (bottom). See Fig. 4 for additional figure descriptions.

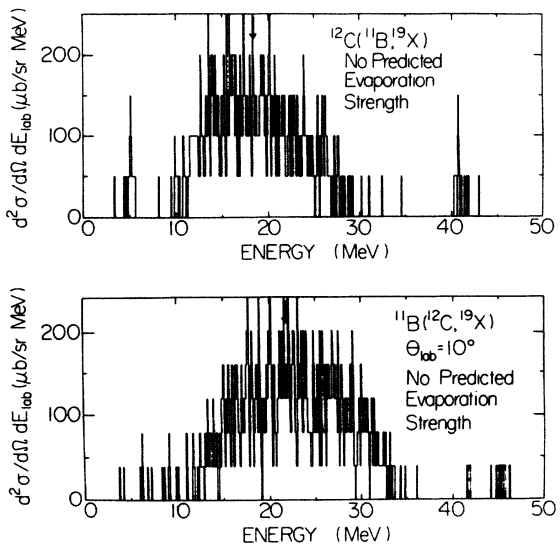

FIG. 10. A comparison of the mass 19 energy spectra for 48 MeV ^{11}B on ^{12}C (top) and 52.36 MeV ^{12}C on ^{11}B (bottom). See Fig. 4 for additional figure descriptions.

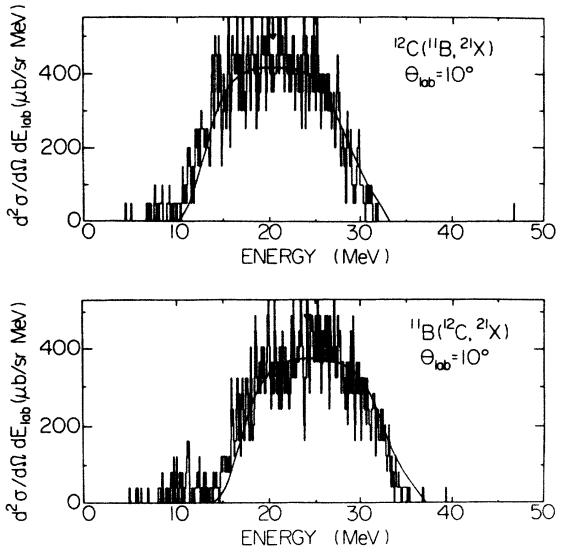

FIG. 12. A comparison of the mass 21 energy spectra for 48 MeV ^{11}B on ^{12}C (top) and 52.36 MeV ^{12}C on ^{11}B (bottom). See Fig. 4 for additional figure descriptions.

tions for masses 15 and 13. In the mass 15 energy spectra, a slightly larger high energy yield exists in the $^{11}B(^{12}C,^{15}X)$ reaction. This increased yield is most prominent at forward angles. By 12° the difference between the $^{12}C(^{11}B,^{15}X)$ and $^{11}B(^{12}C,^{15}X)$ mass 15 energy spectra disappears. The difference in the two energy spectra and the fact that the difference is most prominent at forward angles is, of course, an indication that there is a direct transfer component present in the mass 15 residue. The strength of the additional yield integrated over angle is found to be 5 mb. Such a small cross section has negligible effect on the total fusion cross section and, therefore, would make little difference in the extracted critical angular momentum.

For mass 13, the direct transfer component is readily identifiable at high energies. The strong discrete peaks labeled in Fig. 4 have been kinematically identified. It was argued earlier that the high-energy, direct-transfer recoils would be observed at low energies when the target and projectile were interchanged. This is not the case in Fig. 4 for the mass 13 residues. The discrete states observed in the $^{11}B(^{12}C,^{13}C)^{10}B$ reaction at high ejectile energies are not observed in the mass 13 energy spectrum at low ejectile energies when the target and projectile are interchanged. This is because the recoil energies of these mass 13 residues in the $^{12}C(^{11}B,^{10}B)^{13}C$ reaction are <2 MeV, which puts them below our experimental detection threshold. It should be mentioned that in our original work the

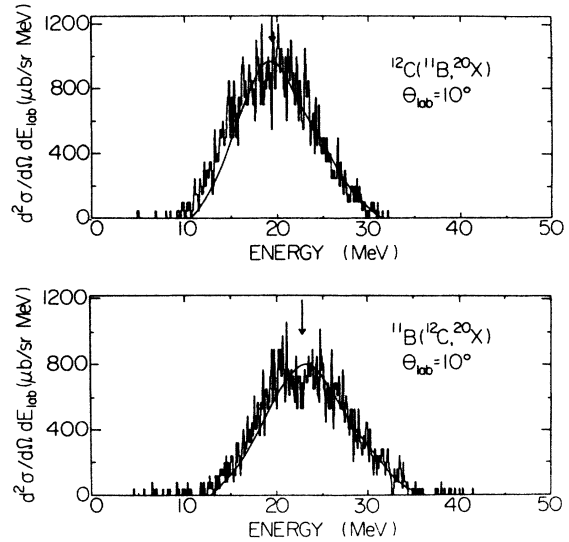

FIG. 11. A comparison of the mass 20 energy spectra for 48 MeV ^{11}B on ^{12}C (top) and 52.36 MeV ^{12}C on ^{11}B (bottom). See Fig. 4 for additional figure descriptions.

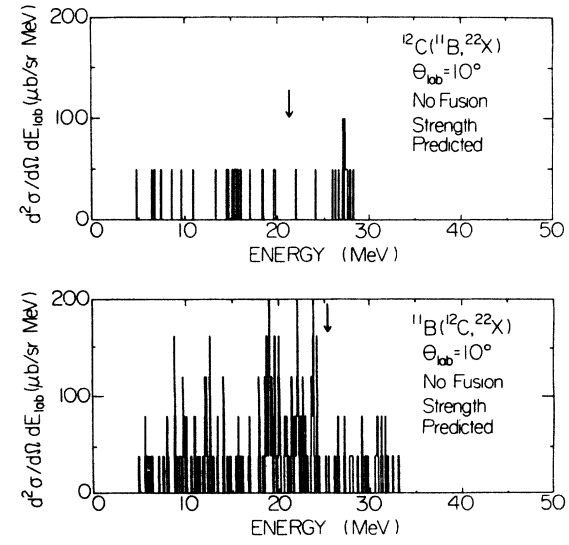

FIG. 13. A comparison of the mass 22 energy spectra for 48 MeV ^{11}B on ^{12}C (top) and 52.36 MeV ^{12}C on ^{11}B (bottom). See Fig. 4 for additional figure descriptions.

yield to the discrete states in the mass 13 energy spectrum was not included in our estimate of the total fusion cross section.

We can now return to our consideration of the possibility that different direct transfer reactions might contribute roughly equally to the energy spectrum of a given mass group when the target and projectile are interchanged. The example discussed earlier involved the $^{12}C(^{11}B,^{15}N)$ alpha-particle pickup and $^{11}B(^{12}C,^{15}N)$ triton pickup reactions. It can be argued that there are no large direct reaction contributions to the mass spectra. The major argument is that all other entrance channels forming the ^{23}Na compound nucleus, i.e., $^{10}B+^{13}C$, $^{9}Be+^{14}N$, and $^{7}Li+^{16}O$,[10,11] exhibit a high energy component in the energy spectrum of the mass 15 residue as shown in Fig. 14. It is extremely unlikely that all four of these entrance channels would contribute significant direct transfer or incomplete fusion strength to this one exit channel. Also, as will be discussed below, the Hauser-Feshbach calculations for fusion evaporation are able to reproduce the shape of the mass 15 energy distribution. While our discussion has focused on the mass 15 residue, similar arguments apply to the other mass groups.

As mentioned previously, Hauser-Feshbach calculations using the computer code LILITA have been made (see Figs. 4–13). To facilitate a comparison of the shapes of the predicted and experimental energy spectra, the calculations have been normalized to the data on a mass-by-mass basis. It should be noted that the calculations were unable to simultaneously reproduce, within a factor of 2, the magnitudes of all the residue strengths. This occurred despite substantial changes in the level density parameters used in the calculation. The calculation was, nevertheless, able to accurately predict the shapes of most of the energy spectra. In particular, the calculation did a good job of predicting the shapes of the energy spectra for masses 15 and 18, the residues whose experimental energy spectra are each characterized by two broad structures. Such structure has been observed and explained in earlier studies of fusion-evaporation reactions in terms of a double solution to the residue velocity vector.[14] This type of structure is particularly prevalent in channels which involve alpha particle emission. In the present experiment, the mass 18 residue most likely results from the emission of an alpha particle and a single nucleon, while the mass 15 residue results from the emission of two alpha particles.

While the calculation was able to reproduce the shapes of most of the residue energy spectra, it did a relatively poor job of predicting the energy distributions of the mass 16 and 17 groups. While we have no good explanation for why the calculation fails for these masses, it may be due, in part, to the fact that a large number of light particles, 4 and 3, must be emitted to reach mass groups 16 and 17, respectively (LILITA assumes only the emission of neutrons, protons, and alpha particles).

The integrated cross sections for the various residues are presented in Table I for the two reactions. For masses 14–22, all of the residue yield in each of the mass groups was used as there was either no evidence or only slight evidence (namely the slight shape difference in the mass 15 energy spectra at forward angles) of any nonfusion strength in the energy spectra of any of these masses. For mass 13, the high energy component was attributed to direct transfer and therefore was not included in the calculation of the fusion-evaporation cross section for that mass. In the $^{12}C(^{11}B,X)$ and $^{11}B(^{12}C,X)$ reactions, the fusion cross sections for the mass 11 and 12 exit channels,

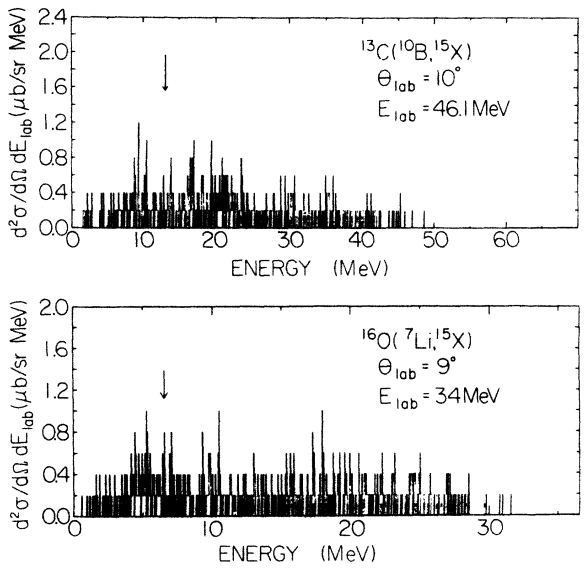

FIG. 14. The mass 15 residue spectra for the reactions $^{13}C(^{10}B,^{15}X)$ and $^{16}O(^{7}Li,^{15}X)$. While better statistics would be desirable, the high energy component seen in the mass 15 spectrum for the $^{12}C(^{11}B,^{15}X)$ reaction in Fig. 6 is still readily apparent in the energy spectra for both of the above entrance channels. The arrows indicate the centroid energies calculated using Eq. (1).

TABLE I. Integrated cross sections for the residues resulting from the $^{12}C(^{11}B,X)$ and $^{11}B(^{12}C,X)$ reactions.

Residue mass	Integrated cross section (mb) $^{12}C(^{11}B,X)$	$^{11}B(^{12}C,X)$
11		72
12	18	
13	22	29
14	189	191
15	227	214
16	124	132
17	170	163
18	116	106
19	16	18
20	68	62
21	39	35
22	4	4
Total	993 (sum of masses 12–22)	1026 (sum of masses 11,13–22)

respectively, were obscured by a strong inelastic component. No reliable fusion cross section could be extracted for either of these exit channels.

For those masses where a comparison can be made, one finds that the integrated cross section for a particular residue formed in the $^{12}C(^{11}B,X)$ reaction is essentially identical to the integrated cross section for that residue in the $^{11}B(^{12}C,X)$ reaction. Of course, this result would be expected whether or not there was a nonfusion component in the residue energy spectra (assuming all yield was above the low-energy threshold of the experimental detection system). The close agreement in the cross sections of the mass 14—22 cross sections simply indicates that the two reaction cross sections have been properly normalized using the previously discussed elastic scattering data. However, as no evidence was found for nonfusion yield from the shapes of the energy spectra for these residues, we believe that these cross sections accurately reflect the fusion strength in these residues. For mass 13, the similarity of the two cross sections after removal of the nonfusion component suggests that the fusion contribution has been reasonably accurately extracted.

In our earlier $^{12}C(^{11}B,X)$ studies,[9-11] a total fusion cross section of 1063 mb was found at 48 MeV when the integrated cross sections for masses 12—22 were summed (the fusion strength of the mass 11 group could not be determined because of a strong inelastic component). The corresponding value in the present study is 993 mb, a value which is well within the experimental uncertainty associated with the two measurements. It should also be kept in mind that the fusion yield to the mass 11 residue has been omitted in the $^{11}B+^{12}C$ experiment while no such omissions were necessary in our studies of the other three entrance channels. In the present study, the mass 11 fusion cross section for the $^{11}B+^{12}C$ entrance channel can be obtained from the $^{11}B(^{12}C,X)$ reaction. A 72 mb cross section is found. This result is in good agreement with the 60 mb mass 11 fusion strength measured in the $^{9}Be+^{14}N$ and $^{7}Li+^{16}O$ studies.[11] The inclusion of this yield brings the total fusion cross section for $^{12}C(^{11}B,X)$ from the present study up to 1065 mb. Thus the present study, like the earlier one, leads to a critical angular momentum for $^{12}C(^{11}B,X)$ fusion reaction which is two units of angular momentum higher than the values found in the $^{13}C(^{10}B,X)$, $^{16}O(^{7}Li,X)$, and $^{9}Be(^{14}N,X)$ investigations.

IV. CONCLUSION

The extraction of critical angular momenta from fusion-evaporation cross sections is meaningful only if the fusion strength has been properly identified. Of primary concern in such studies is the incorrect identification of products due to such processes as direct transfer and incomplete fusion, as fusion-evaporation events. This question has been of particular importance in our earlier study of the four entrance channels which form the ^{23}Na compound nucleus. In that work the critical angular momenta extracted from the fusion cross sections for each of the four entrance channels did not approach a common limitation with increasing bombarding energy. This ruled out a limitation in the fusion cross section based upon having reached a critical density of states in the compound nucleus. This conclusion assumes that the fusion cross section has been properly identified and that the critical angular momenta are indeed correct. The present study again looks at the $^{11}B+^{12}C$ fusion cross section in an effort to verify that no nonfusion yield was included in the fusion cross section for this channel in our earlier work. We have exploited the fact that the energy of direct transfer and incomplete fusion yield depends strongly on the entrance channel configuration, i.e., $^{12}C(^{11}B,X)$ or $^{11}B(^{12}C,X)$, and that the energy of fusion residues does not. In our current search no evidence of a significant nonfusion yield was found in any of the previously measured $^{11}B+^{12}C$ residue cross sections. As there is no change in the fusion cross section and, therefore, no change in the critical angular momenta, our earlier conclusion that a critical density of compound nuclear states is not responsible for the observed fusion cross section limitation remains unchanged.

ACKNOWLEDGMENTS

It is a pleasure to acknowledge the many productive discussions the authors have had during the course of this work with Dr. Larry Dennis. In addition, the authors would like to thank Tennessee Tech students, Greg Gentry, Dale Baltimore, and John Kozub, for their assistance in data acquisition and analysis. This work was supported in part by the Division of High Energy and Nuclear Physics, U.S. Department of Energy under Contract No. DE-AS05-80ER10714, and by the National Science Foundation.

[1]R. Bass, Phys. Rev. Lett. **39**, 265 (1977).

[2]D. Horn and A. J. Ferguson, Phys. Rev. Lett. **41**, 1529 (1978).

[3]D. G. Kovar, D. F. Geesaman, T. H. Braid, Y. Eisen, W. Henning, T. R. Ophel, M. Paul, K. E. Rehm, S. J. Sanders, P. Sperr, J. P. Schiffer, S. L. Tabor, S. Vigdor, and B. Zeidman, Phys. Rev. C **20**, 1305 (1979), and references therein.

[4]J. Gomez del Campo, R. A. Dayras, J. A. Biggerstaff, D. Shapira, A. H. Snell, P. H. Stelson, and R. G. Stokstad, Phys. Rev. Lett. **43**, 26 (1979).

[5]J. P. Wieleczko, S. Harar, M. Conjeaud, and F. Saint-Laurent, Phys. Lett. **93B**, 35 (1980).

[6]F. Saint-Laurent, M. Conjeaud, and S. Harar, Nucl. Phys. **A327**, 517 (1979).

[7]S. M. Lee, T. Matsuse, and A. Arima, Phys. Rev. Lett. **45**, 165 (1980).

[8]L. C. Dennis and S. T. Thornton, Phys. Rev. C **22**, 340 (1980).

[9]J. F. Mateja, A. D. Frawley, L. C. Dennis, K. Abdo, and K. W. Kemper, Phys. Rev. Lett. **47**, 311 (1981).

[10]J. F. Mateja, A. D. Frawley, L. C. Dennis, K. Abdo, and K. W. Kemper, Phys. Rev. C **25**, 2963 (1982).

[11]J. F. Mateja, J. Garman, D. E. Fields, R. L. Kozub, A. D. Frawley, and L. C. Dennis, Phys. Rev. C **30**, 134 (1984).
[12]A. D. Frawley, J. F. Mateja, A. Roy, and N. R. Fletcher, Phys. Rev. Lett. **41**, 846 (1978).
[13]J. Gomez del Campo and R. G. Stokstad, Oak Ridge National Laboratory Report No. ORNL/TM-7295, 1981.
[14]J. Gomez del Campo, R. G. Stokstad, J. A. Biggerstaff, R. A. Dayras, A. H. Snell, and P. H. Stelson, Phys. Rev. C **19**, 2170 (1979).